International Journal of Engineering, Mathematical and Physical Sciences
ISSN: 2517-9934
Vol:7, No:8, 2013

Slip Effect Study of 4:1 Contraction Flow for Oldroyd-B Model

N. Thongjub, B. Puangkird, and V. Ngamaramvaranggul

***Abstract*—**The numerical simulation of the slip effect via vicoelastic fluid for 4:1 contraction problem is investigated with regard to kinematic behaviors of streamlines and stress tensor by models of the Navier-Stokes and Oldroyd-B equations. Two-dimensional spatial reference system of incompressible creeping flow with and without slip velocity is determined and the finite element method of a semi-implicit Taylor-Galerkin pressure-correction is applied to compute the problem of this Cartesian coordinate system including the schemes of velocity gradient recovery method and the streamline-Upwind / Petrov-Galerkin procedure. The slip effect at channel wall is added to calculate after each time step in order to intend the alteration of flow path. The result of stress values and the vortices are reduced by the optimum slip coefficient of 0.1 with near the outcome of analytical solution.

***Keywords*—**Slip effect, Oldroyd-B fluid, slip coefficient, time stepping method.

I. Introduction

THIS article is concentrated upon the application of the slip effect for Oldroyd-B constitutive model in the field of 4:1 contraction flows to adopt a semi-implicit Taylor-Galerkin pressure-correction finite element method (STGFEM) as a tool for solving a problem for this flow. The influence of shear stress in sharp corner 4:1 contraction domains is analyzed and corrected by adding the slip function on the boundary of channel wall.

The 4:1 contraction flow is a well know problem to study kinematic behavior of viscoelastic flows whilst flow path has sudden change in the kind of this geometry especially for two-dimensional system. There are strong elongation and violent shear stress at contraction position. The experimental work, Walters and Rawlinson [1] have set up the experiment of planar contraction flows for Boger fluid. Boger [2] has solved the numerical solution of circular contraction for both Newtonian and Non-Newtonian fluids and the comparison with the experimental result has been presented in 1987.

Instead of solving analytic solution of viscoelastic problem through which it is extremely hard to find the non-linear partial differential equations in the mathematical model of the conservation of mass and momentum equations (including constitutive equation); one can utilize the numerical techniques which can efficiently eliminate inconvenient problems. n this fashion, there are variety numerical schemes such as finite difference method (FDM), finite volume method (FVM) and finite element method (FEM) to calculate the approximate solution together with non-significant error. In 1999, Phillips and Williams [3] have taken a semi-Lagrangian FVM to solve a 4:1 planar contraction of Oldroyd-B fluid for creeping and inertial flows. Shortly after, they [4] have typically using different data of the same problem by expanding a new axisymmetric flow but this time the grids have been fixed in Eulerian methods. Aboubacar et al. [5], [6] have shown that the technique of a cell-vertex hybrid finite volume/element method is appropriate to compute highly elastic solutions for Oldroyd-B and Phan-Thien/Tanner (PTT) fluids with both rounded and sharp corner contraction figures. Alves et al. [7] have selected the FVM to calculate creeping PTT flow past planar abrupt contractions and make clear that Deborah numbers and contraction ratios are dependent on flow characteristics.

There are a number of problems that have been solved by FEM. In 2001, Ngamaramvaranggul and Webster [8] have applied FEM for Oldroyd-B problem of stick-slip flow and they modified the top boundary after die exit by free surface method in order to develop this flow to Die-swell flow and they found that swelling ratio is varied as a function of relaxation time. Consequently, they [9] have simulated a problem of pressure-tooling wire-coating flows with Phan-Thien/Tanner fluid via employment of the same standard of FEM and streamline-upwind Petrov/Galerkin (SUPG) to stabilized the converge solution.

Comparing experimental and numerical results for fluid flows through solid wall help us to contemplate the speed of fluid particles those which are not only stick but also slip on solid surface. Hence, a great number of recent scientific researchers have documented various methods to estimate slip velocity at compact boundary. A numerical study of Newtonian and viscoelastic flow on slip effect for free surface has been presented by Silliman and Scriven [10]. This result got along well with the next experiment of Ramamurthy [11] who has focused on surface melt fracture of HDPE and LLDPE that is the outcome from slip in die land. Previously, both slip cases had been sustained greatly with analysis solution of Jiang et al. [12] by setting slip velocity for capillary tubes as a function of wall shear stress as well as Phan-Thien [13] who demonstrated the same concept of slip

N. Thongjub is in the Department of Mathematics and Computer Science, Faculty of Science, Chulalongkorn University, Bangkok 10330, Thailand (phone: +668 6767 5029; fax: +662 255 2287; e-mail: t_nawalax@hotmail.com).

B. Puangkird is in the Department of Mechanical Engineering, Faculty of Engineering, King Mongkut's Institute of Technology Ladkrabang (KMITL), Bangkok 10520, Thailand (phone: +668 5364 3410; fax: +662 255 2287; e-mail: kpbumroo@kmitl.ac.th).

V. Ngamaramvaranggul is with the Department of Mathematics and Computer Science, Faculty of Science, Chulalongkorn University, Bangkok 10330 Thailand Corresponding author: (phone: +668 6031 9699; fax: +662 255 2287; e-mail: vimolrat.n@chula.ac.th).

velocity and found that slip velocity still be observed while the critical shear stress is less than wall shear stress. In 2000, Ngamaramvaranggul and Webster [14] have stated various slip effect schemes to consider the free surface in tube-tooling and pressure-tooling die problems.

In this research, the slip effect scheme has been determined in the problem of 4:1 contraction for Newtonian and Oldroyd-B fluids under the two-dimensional planar isothermal incompressible flow and formed the mathematical model of Navier-Stokes equations by means of STGFEM. Simultaneously, the velocity gradient recovery and the streamline-upwind Petrov/Galerkin techniques have been chosen to stabilize the converged solutions. Finally, the solutions have been considered no slip case and slip condition in an attempt to find the optimal slip coefficient for each fluid with sharp corner geometries illustrated.

II. Governing Equations

The conservation of mass and momentum for incompressible isothermal viscoelastic flow without gravity is maintained in term of Navier-Stokes equations. In this work, the dimensionless equations as the derivative model of continuity equation (1) and kinematic equation (2). Especially for equation motion (2), the particular non-dimensional Reynolds number (Re) is revealed. For creeping flow, $Re = 0$.

$$\nabla \cdot \vec{U} = 0 \tag{1}$$

$$Re\vec{U}_t = \nabla \cdot \boldsymbol{T} - Re\vec{U} \cdot \nabla \vec{U} - \nabla \vec{P} \tag{2}$$

where ∇ is the differential operator, $\vec{U}$ is velocity vector, $Re = \dfrac{\rho VL}{\mu_0}$, $\vec{U}_t$ is time derivative of $\vec{U}$, $\vec{P}$ is pressure, and the extra-stress tensor $\boldsymbol{T} = \boldsymbol{\tau} + 2\mu_2 \boldsymbol{D}$, $\boldsymbol{\tau}$ is the polymeric component of the extra-stress tensor, the rate of deformation tensor $\boldsymbol{D} = \dfrac{\left(\nabla \vec{U} + \left(\nabla \vec{U}\right)^{\mathrm{T}}\right)}{2}$, the transpose operator is $(\ )^{\mathrm{T}}$. Here, ρ is the fluid density, V is the characteristic velocity, L is the characteristic length in terms of channel width and μ_0 is the zero-shear viscosity which $\mu_0 = \mu_1 + \mu_2$ where μ_1 is the polymeric viscosity and μ_2 is the solvent viscosity. The non-dimensional parameters are $\mu_1 / \mu_0 = 0.88$ and $\mu_2 / \mu_0 = 0.12$.

The non-dimensional constitutive equation of a viscoelastic fluid for Oldroyd-B model is

$$We\boldsymbol{\tau}_t = 2\mu_1 \boldsymbol{D} - \tau + We\left[\boldsymbol{\tau} \cdot \nabla \vec{U} + \left(\nabla \vec{U}\right)^T \cdot \boldsymbol{\tau} - \vec{U} \cdot \nabla \boldsymbol{\tau}\right] \tag{3}$$

where We is the non-dimensional Weissenberg number, $We = \lambda_1 \dfrac{V}{L}$, and λ_1 is the relaxation time.

For convenience to calculate the shear stress (τ_{xy}) of Oldroyd-B fluid, Johnson and Segalman [15] have applied shear stress as a function of shear viscosity (η) and shear rate $(\dot{\gamma})$ on the basis of the kinematic theory of macro-molecules.

$$\tau_{xy} = \frac{\eta_1 \dot{\gamma}}{1 + a(2-a)\,(\lambda_1\, \dot{\gamma})^2} + \eta_2 \dot{\gamma} \tag{4}$$

where η_1 and η_2 are viscosity coefficients and a is a scalar parameter between (0, 2).

III. Numerical Scheme

The non-linear differential equations (2) and (3) are difficult to solve by analysis method so we have utilized numerical technique to perform on standard FEM. The convection terms of Navier- Stokes equation (2) and the constitutive equation of Oldroyd-B model (3) are controlled to calculate by means of below scheme STGFEM that is a method to split both the equations into half time step. Since the continuous equations (2) and (3) are converted to discretization equations and formulated to system of linear equation, the approximate solution is computed with Jacobi iterative method and Cholesky decomposition scheme.

A. Semi-Implicit Taylor-Galerkin Pressure-Correction Finite Element Method

To solve convection equations conveniently, the perfect union of factional time steps and FEM is employed to separate non-dimensional (2) and (3) for three stages per time step as below classification. This accumulation technique is known as semi-implicit Taylor-Galerkin pressure-correction finite element method.

Step 1a:

$$\left(2\frac{Re}{\Delta t}\right)\left(\vec{U}^{n+1/2} - \vec{U}^{n}\right) = \left(\nabla \cdot \left(\boldsymbol{\tau} + 2\mu_2 \boldsymbol{D}\right) - Re\vec{U} \cdot \nabla \vec{U} - \nabla \vec{P}\right)^n + \nabla \cdot \mu_2 \left(\boldsymbol{D}^{n+1/2} - \boldsymbol{D}^{n}\right) \tag{5}$$

$$\left(2\frac{We}{\Delta t}\right)\left(\boldsymbol{\tau}^{n+1/2} - \boldsymbol{\tau}^{n}\right) = We\left(\boldsymbol{\tau} \cdot \nabla \vec{U} + \left(\nabla \vec{U}\right)^{\mathrm{T}} \cdot \boldsymbol{\tau} - \vec{U} \cdot \nabla \boldsymbol{\tau}\right)^n + \left(2\mu_1 \boldsymbol{D} - \boldsymbol{\tau}\right)^n \tag{6}$$

Step 1b:

$$\left(\frac{Re}{\Delta t}\right)\left(\bar{U}^{*}-\bar{U}^{n}\right)=\left(\nabla\cdot\boldsymbol{\tau}-Re\bar{U}\cdot\nabla\bar{U}\right)^{n+1/2}+\nabla\cdot\mu_2\left(\boldsymbol{D}^{*}-\boldsymbol{D}^{n}\right)$$
$$+\left(\ \nabla\cdot\left(2\mu_2\boldsymbol{D}\right)-\nabla\bar{P}\right)^{n} \quad (7)$$

$$\left(\frac{We}{\Delta t}\right)\left(\boldsymbol{\tau}^{n+1}-\boldsymbol{\tau}^{n}\right)=We\left(\boldsymbol{\tau}\cdot\nabla\bar{U}+\left(\nabla\bar{U}\right)^{\mathrm{T}}\cdot\boldsymbol{\tau}-\bar{U}\cdot\nabla\boldsymbol{\tau}\right)^{n+1/2}$$
$$+\left(2\mu_1\boldsymbol{D}-\boldsymbol{\tau}\right)^{n+1/2} \quad (8)$$

Step 2:

$$\nabla^2\left(\bar{P}^{n+1}-\bar{P}^{n}\right)=\left(2Re/\Delta t\right)\nabla\bar{U}^{*} \quad (9)$$

Step 3:

$$\left(2\frac{Re}{\Delta t}\right)\left(\bar{U}^{n+1}-\bar{U}^{*}\right)=-\left(\bar{P}^{n+1}-\bar{P}^{n}\right) \quad (10)$$

The partial differential equations (5)-(10) are discretised with FDM and FEM. The left for time derivative term is used the Taylor series and the right for spatial component is adopt the weight residual of Galerkin finite element method so the equations of stages (1)-(3) are converted to the system of linear equations. The geometrical area of flow is generated to small triangular element mesh in order to get the precise solution before approximate solution is solved with Jacobi iterative method for steps 1 and 3, and Cholesky decomposition for step 2.

B. Phan-Thien Slip Rule

To reduce shear stress at sharp corner point, Phan-Thien [13] have presented the slip at solid wall by setting the slip velocity as a function of wall shear stress so the result is more precisely close to the same problem of experimental outcome. The slip velocity will be computed if some values of wall shear stress are greater than a constant critical shear value.

$$V_{slip}=V_{mean}\left(1-exp\left(-\alpha\boldsymbol{\tau}/\boldsymbol{\tau}_{crit}\right)\right) \quad (11)$$

where V_{slip} is the slip velocity, V_{mean} is the mean velocity flowrate for no slip case, α is the constant slip coefficient, $\boldsymbol{\tau}$ is the wall shear stress and $\boldsymbol{\tau}_{crit}$ is the critical shear stress.

IV. Problem Specification

There is a benchmark of slip and no slip cases in the same geometrical domain for 4:1 contraction flows that is normally used in industrial processes so the major body is picked in the model of sharp corner shape. The geometry of planar 4:1 contraction especially by focusing on the downstream half channel width L at entry and exit sections of $27.5L$ and $49L$ respectively is displayed in Fig. 1.

The upstream inlet length is imposed to Poiseuille flow and fluid passes in channel, which is long enough to complete developing flow so the downstream exit length is still maintaining parabolic flow. At the channel wall, the slip condition is applied to obtain intensive outcome close on real problem.

$$u(y)=3(16-y^2)/128,\quad v=0 \quad (12)$$

$$\tau_{xx}=2We\,\mu_1\left(\frac{\partial u}{\partial y}\right)^2,\quad \tau_{yy}=0,\ \text{and}\ \tau_{xy}=\mu_1\frac{\partial u}{\partial y}.$$

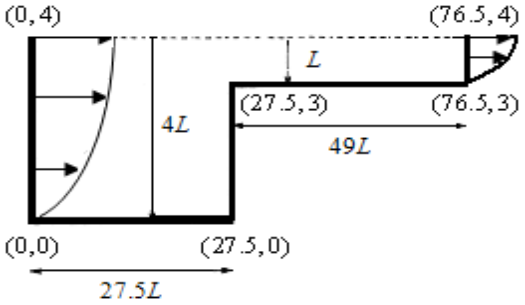

Fig. 1 Schematic of 4:1 contraction flow

TABLE I
Mesh Characteristics

Meshes	Elements	Nodes	Degree of Freedom	h_{min}
mesh1	980	2105	11088	0.025
mesh2	1140	2427	12779	0.023
mesh3	2987	6220	32717	0.006
mesh4	5140	10575	55593	0.004

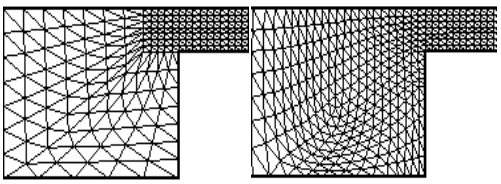

(a) mesh1 (b) mesh2

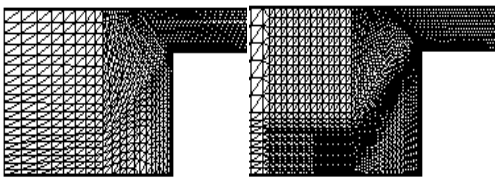

(c) Mesh3 (d) mesh4

Fig. 2 Mesh pattern of 4:1 contraction flow

To inspect the severe stress at impact wall, the sharp corner contraction mesh1- mesh4 are determined in four delicate

order grids of very coarse, coarse, medium and fine meshes which were used by Aboubacar et al. [5] as illustrated in Table I and Fig. 2. All meshes are bias and the tiny elements ($h_{\min}$) are placed next to the singularity.

V. Results

The results of sharp corner meshes are considered and the best mesh is chosen to run for final solution in order to reduce duplicate outcome. After optimal mesh was taken, it was brought to run in both Newtonian and viscoelastic fluids under the condition of no slip and slip effect. The slip coefficients for each liquid are determined to adjust the flow pattern as displayed below.

A. Newtonian Fluid

The peak values on bottom downstream wall with no slip of normal stress τ_{xx} and τ_{yy}, shear stress τ_{xy} and shear rate $\dot{\gamma}$ in Table II grow upon higher sensitivity of grid and we observed that the peak of all values can classified in two groups of resemblance. The results for mesh1 and mesh2 of first group are similar as well as the next group of mesh3 and mesh4 but the outcomes of the second group are conspicuous.

TABLE II
The Peak Values of Newtonian Fluid on Bottom Downstream Wall with No Slip

Meshes	τ_{xx}	τ_{xy}	τ_{yy}	$\dot{\gamma}$
mesh1	9.046	4.523	0.335	4.832
mesh2	9.014	4.507	0.330	4.753
mesh3	12.488	6.244	0.328	6.597
mesh4	15.998	8.000	0.325	8.660

In order to choose a suitable mesh to get the final solution, the dominant mesh will be picked, that is mesh3 or mesh4. For this case mesh3 is the best choice to prompt display even if mesh4 is fine net structure because the result of mesh3 can be run easier and faster to get converged solution than mesh4 whilst both grids give the little difference so the minor error can be negligible.

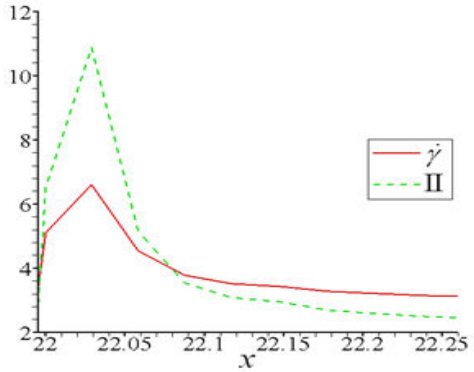

Fig. 3 II and $\dot{\gamma}$ along bottom downstream wall with no slip of Newtonian fluid

The similar behavior of second invariant (II) and shear rate ($\dot{\gamma}$) of Newtonian fluid for mesh3 are displayed in Fig. 3. Both curves for II and $\dot{\gamma}$ look like a left-skewed distribution and the peaks are 10.881 and 6.597 for II and $\dot{\gamma}$, respectively. From the previous work, we found that all apexes go to singularity in case of high We and these values are remote from physical phenomena so this is the reason to reduce the zenith with slip condition as see in Fig. 4.

For selecting the optimum value of α and the critical II (II_{crit}), we utilized mesh3 to execute the slip effect for Newtonian fluid by running α from 0.1 to1 as illustrated in Fig. 5. First round of computation to find minimum α of fixing $\text{II}_{crit} = 2.3$ for α at 0.3, 0.5, and 1 is noticed that oscillations appear distinctly but $\alpha = 0.1$ is ascertained properly the value of lowest peak $\dot{\gamma}$. This selection of minimum $\dot{\gamma}$ is supported by Fig. 5 which presents a correlation between $\dot{\gamma}$ and α. Second round of calculation to find the location of II_{crit} by setting $\alpha = 0.1$ and altering II_{crit} from 0 to 10 is operated before relation of $\dot{\gamma}$ versus II_{crit} shows that the lowest II_{crit} points to 2.3 in Fig. 6.

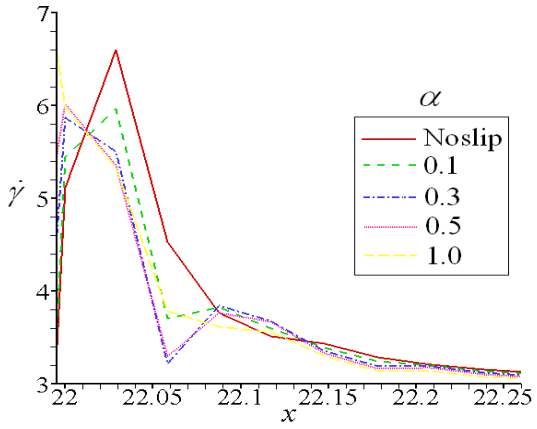

Fig. 4 $\dot{\gamma}$ of various α along bottom downstream wall of Newtonian fluid at II = 2.3

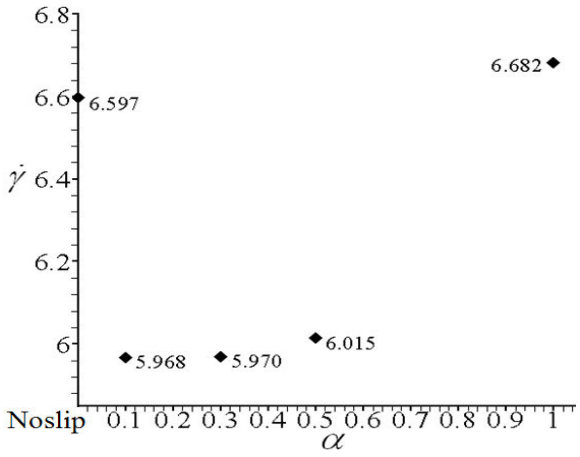

Fig. 5 The peak of $\dot{\gamma}$ versus α on bottom downstream wall of Newtonian fluid at $\mathrm{II} = 2.3$

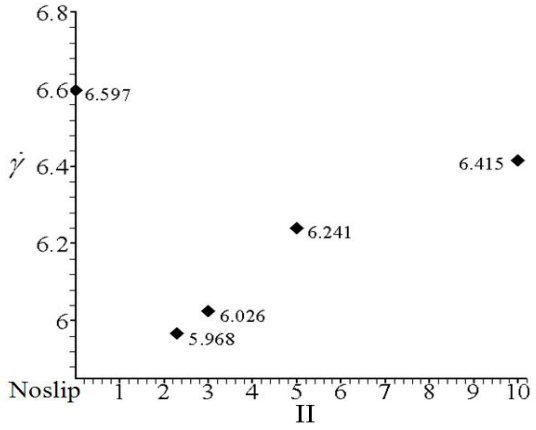

Fig. 6 The peak of $\dot{\gamma}$ versus II_{crit} on bottom down-stream wall of Newtonian fluid at $\alpha = 0.1$

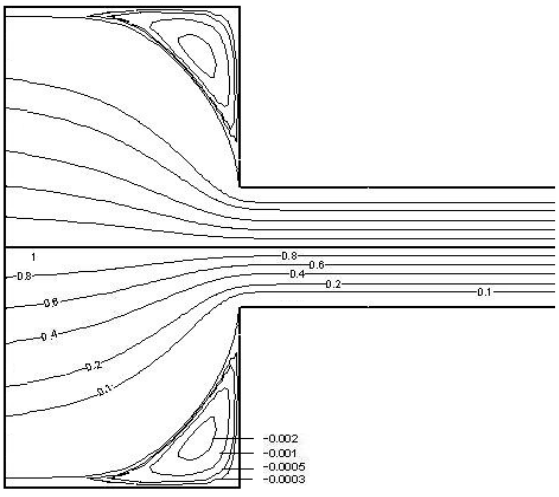

(a) no slip

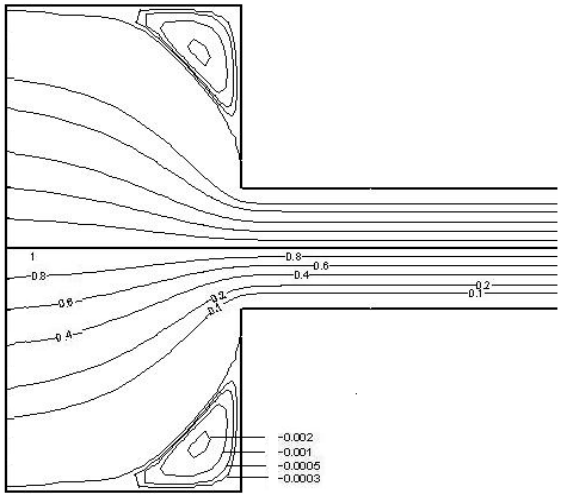

(b) slip at $\alpha = 0.1$ and $\mathrm{II} = 2.3$

Fig. 7 S line contour of Newtonian fluid

Fig. 7 manifests streamline (S) line contour for no slip in Fig. 7 (a) and slip effect at $\alpha = 0.1$, $\mathrm{II} = 2.3$ in Fig. 7 (b). Graphs of both cases look alike but the vortex at the corner of no slip is bigger than that of its counterpart in the slip case.

B. Viscoelastic Fluid

For all sharp corner meshes in Table III, the viscoelastic fluids are considered for various We. The peak values on bottom downstream wall with no slip of normal stress $\dot{\gamma}$ grow upon high We and we noticed that the peak of $\dot{\gamma}$ for all meshes have increased with the same trend. The results of group one for mesh1 and mesh2 are identical as well as group two of mesh3 and mesh4 but the consequence of second group is prominent. Since the tendency of behavior for all We has the same direction, all sharp meshes are illustrated only $We = 1$ for all stresses $(\tau_{xx}, \tau_{xy}, \tau_{yy})$ with the same condition in Table IV. Mesh3 is chosen to run for the final solution for the same reasons stated earlier. So Figs. 8-12 in this item are the results obtained for this mesh.

TABLE III
THE PEAK VALUES OF $\dot{\gamma}$ ON BOTTOM DOWNSTREAM WALL WITH NO SLIP OF OLDROYD-B FLUID

Meshes	0.25	0.5	0.75	1
mesh1	4.873	5.130	5.323	5.717
mesh2	4.929	5.061	5.153	5.510
mesh3	7.534	8.550	8.828	9.204
mesh4	8.833	9.380	9.504	10.234

TABLE IV
THE PEAK VALUES OF STRESS τ_{xx}, τ_{xy} AND τ_{yy} ON THE BOTTOM DOWNSTREAM WALL WITH NO SLIP OF OLDROYD-B FLUID AT $We = 1$

Meshes	τ_{xx}	τ_{xy}	τ_{yy}
mesh1	21.458	7.236	2.507
mesh2	22.512	8.047	3.018
mesh3	36.571	15.496	6.427
mesh4	37.670	15.068	8.772

To select critical II from Fig. 8, we have determined the optimum α for We=0.25 before calculation of high We via varying all α values between 0.1 and 1 so $\text{II} = 14$ is set first because the shear rate is high enough to switch some stick velocities to move freely. For selecting proper α by minimizing shear rate, the same procedure of Newtonian case is operated as shown in Fig. 9 so the minimum shear rate is 7.530 at $\alpha = 0.1$ that is under the value of no slip condition while the other value of α has gone beyond the value of slip case. Other α values are rejected except $\alpha = 0.1$ since the slip velocity reduces shear rate. By adjusting critical II, the range of II is started at 5 to 14 since the off range cannot be calculated for $\alpha = 0.1$ but the range II that is shown in Fig. 10 and the least value shear rate for $\text{II} = 6$ is 7.175; therefore, the suitable coefficient slip is 0.1.

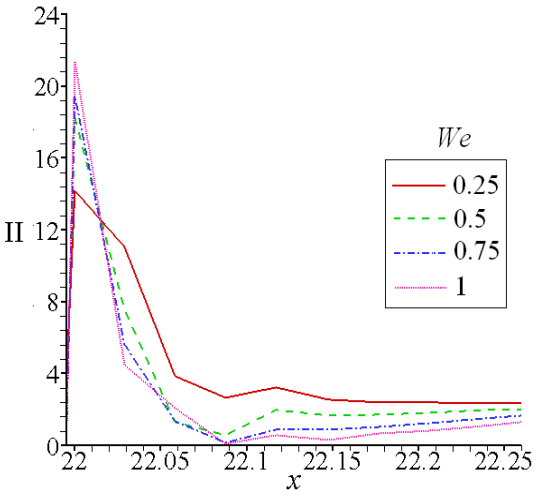

Fig. 8 II on the bottom downstream wall with no slip of Oldroyd-B fluid

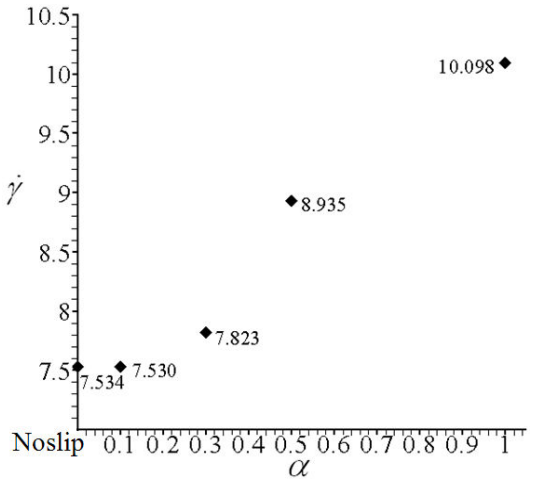

Fig. 9 The peak of $\dot{\gamma}$ versus α on bottom downstream wall of Oldroyd-B fluid at We=0.25

TABLE V
THE LOWEST SHEAR RATE FOR PROPER α AND SUITABLE II OF OLDROYD-B FLUID

We	0	0.25	0.5	0.75	1
II_{crit}	2.3	6	4	3.5	3.3
$\dot{\gamma}$	5.968	7.175	7.554	8.611	8.801
α	0.1	0.1	0.1	0.1	0.1

TABLE VI
THE PEAK VALUE OF $\dot{\gamma}$ AND τ_{xx} ON THE BOTTOM DOWNSTREAM WALL

We	$\dot{\gamma}$		τ_{xx}	
	No Slip	Slip	No Slip	Slip
0.25	7.534	7.175	19.943	13.494
0.5	8.550	7.554	29.455	20.586
0.75	8.828	8.611	34.042	30.975
1	9.253	8.721	36.571	34.557

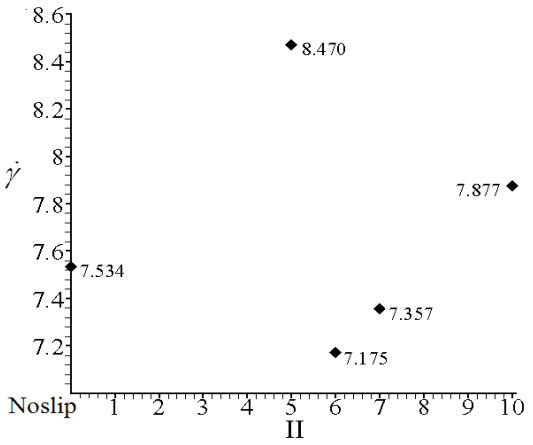

Fig. 10 The peak of $\dot{\gamma}$ versus II_{crit} on bottom downstream wall of Oldroyd-B fluid at We=0.25

Similarly, the lowest shear rates of We = 0.5, 0.75, and 1 for fitting critical II are shown in Table V.

Epitomizing the highest τ_{xx} and the maximum shear rate values of the optimum slip velocity in Table VI are less than the maximum values of no slip condition for a sharp corner domain. The maximum value of τ_{xx} is reduced from 19.943 to 13.494 and the peak of $\dot{\gamma}$ is decreased from 7.534 to 7.1745 at $We = 0.25$. Similar to the trend of the slip influence for We at 0.5, 0.75 and 1, the maximum of $\dot{\gamma}$ and τ_{xx} without slip falls below that for the case with slip. Highly reducing the stress value is clearly investigated, refer to Table VI.

If we compare the streamline of Fig. 11 (a) for no slip and Fig. 11 (b) for slip, the serious vortex is simple notice for no slip case so this remark can get along well with Newtonian behavior.

Fig. 12 is the graphs of benchmarks in shear stress τ_{xy} versus shear rate $\dot{\gamma}$ of J&S (Johnson-Segalman) theory from (4) with two restriction flows under condition of no-slip and slip along bottom downstream wall at We=0.25 in Fig. 12 (a) and $We = 1$ in Fig. 12 (b). This plot is indicative of the fact that the shear stress of both cases agree in trend along the resistance but slip limitation is closer to J&S though the value of prediction is slightly undershoot.

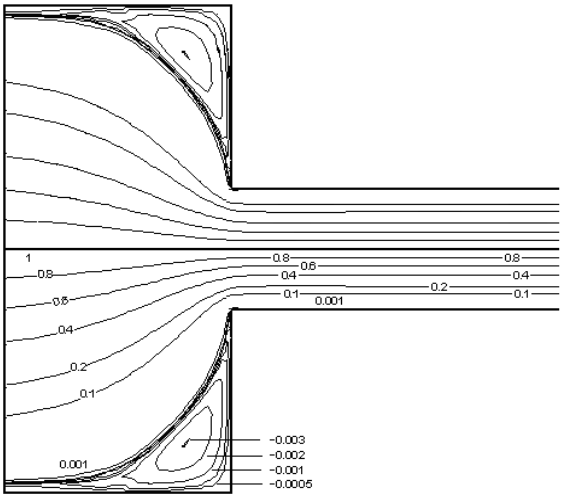

(a) no slip

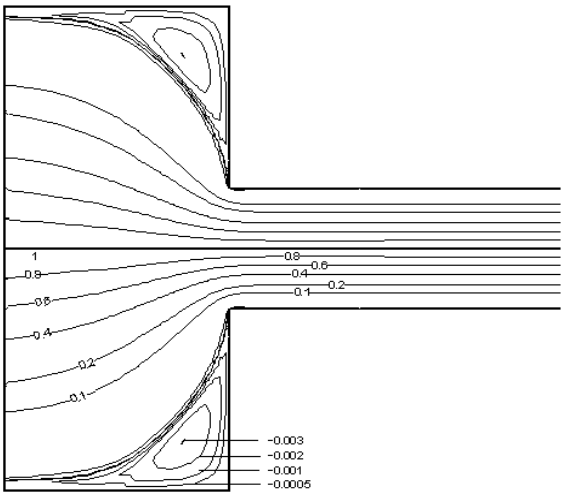

(b) slip at $\alpha = 0.1$ and $\mathrm{II} = 3.3$

Fig. 11 S line contour of Oldroyd-B at $We = 1$

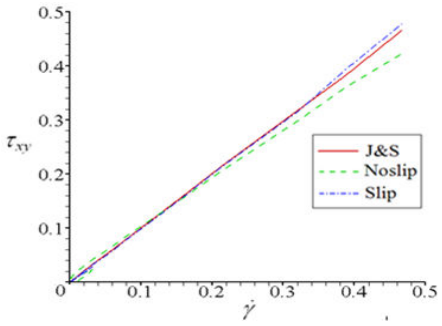

(a) $We = 0.25$

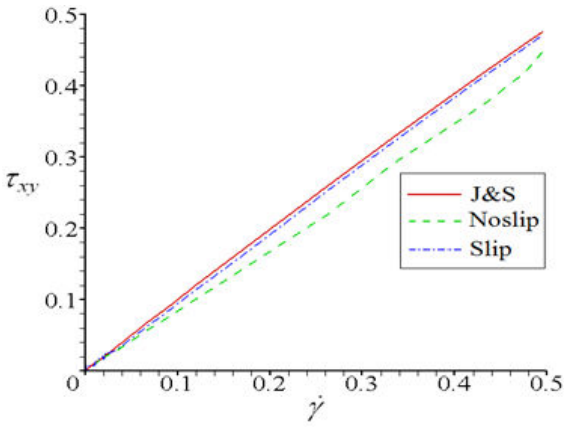

(b) $We = 1$

Fig. 12 The comparison of τ_{xy} versus $\dot{\gamma}$ with J&S on bottom downstream wall of Oldroyd-B fluid

VI. Conclusion

For the outcomes of slip effect in 4:1 contraction problem, we found that the optimum slip coefficient for sharp corner

meshes of all We is 0.1 if we adjust the proper critical II. The appropriate values of the slip coefficient and the second invariant cause the peak of shear rate lower than no-slip case.

Hence it can be concluded that the slip well reduces the stress along the wall. In the same direction, when the small We is input, the less effect is appeared and this is reversed with high Weissenberg numbers.

ACKNOWLEDGMENT

The authors would like to thank the scholarship from National Science and Technology Development Agency (NSTDA), Thailand to support PhD degree and Advanced Virtual and Intelligence Computing (AVIC) at the Department of Mathematics and Computer Science, Faculty of Science, Chulalongkorn University to sustain the advanced computer machinery.

REFERENCES

[1] K. Walters, D. M. Rawlinson, On some contraction flows for Boger fluid, Rheol. Acta., vol 21, pp. 547-552, 1982.
[2] D.V. Boger, Viscoelastic flows through contractions, Ann. Rev. Fluid Mech., vol 19, pp. 157–182, 1987.
[3] T.N. Phillips, A.J. Williams, Viscoelastic flow through a planar contraction using a semi-Lagrangian finite volume method, J. Non-Newtonian Fluid Mech., vol 87, pp. 215–246, 1999.
[4] T.N. Phillips, A.J. Williams, Comparison of creeping and inertial flow of an Oldroyd B fluid through planar and axisymmetric contractions, J. Non-Newtonian Fluid Mech., vol 108, pp. 25–47, 2002.
[5] M. Aboubacar and M.F. Webster, "A cell-vertex finite volume/element method on triangles for abrupt contraction viscoelastic flows", J. Non-Newtonian Fluid Mech., vol 98, pp. 83–106, 2001.
[6] M. Aboubacar, H. Matallah, M.F. Webster, Highly elastic solutions for Oldroyd-B and Phan-Thien/Tanner fluids with a finite volume/element method: planar contraction flows, J. Non-Newtonian Fluid Mech., vol 103, pp. 65–103, 2002.
[7] M.A. Alves, D. Torres, M.P. Goncalves, P.J. Oliverira, F.T. Pinho, On the effect of contraction ratio in viscoelastic flow through abrupt contractions, J. Non-Newtonian Fluid Mech., vol 122, pp. 117–130, 2004.
[8] V. Ngamaramvaranggul, M. F. Webster, Viscoelastic simulation of stick-slip and die-swell flows, Int. J. Num. Meth. Fluids, vol 36, pp. 539-595, 2001.
[9] V. Ngamaramvaranggul and M. F. Webster, Simulation of pressure-tooling wire-coating flows with Phan-Thien/Tanner models Int. J. Num. Meth. Fluids, vol 38, pp. 677-710, 2002.
[10] W. J. Silliman, L. E. Scriven, Separating flow near a static contact line: Slip at a wall and shape of a free surface, J. Comp. Phys., vol 34, pp. 287-313, 1980.
[11] A. V. Ramamurthy, Wall slip in viscous fluids and influence of materials of construction, J. Rheol., vol 30, pp. 337-357, 1986.
[12] T. Q. Jiang, A. C. Young, A. B. Metzner, The rheological characterization of HPG gels: Measurement of slip velocity in capillary tubes, Rheol. Acta, vol 25 no.4 , pp. 397-404, 1986.
[13] N. Phan-Thien, Influence of wall slip on extrudate swell: a boundary element investigation, J. Non-Newtonian Fluid Mech., vol 26, pp. 327-340, 1988.
[14] V. Ngamaramvaranggul, M. F. Webster, Simulation of coating flows with slip effects, Int. J. Num. Meth. Fluids. vol 33, pp. 961-992,2000.
[15] M.W. Johnson, D. Segalman, A model for viscoelastic fluid behavior which allows non-affine deformation, J. Non-Newtonian Fluid Mech., vol 2 pp. 255-270, 1977.

N. Thongjub has been studying for Doctoral degree at Department of Mathematics and Computer Science, Faculty of Science, Chulalongkorn University. She has gotten scholarship from National Science and Technology Development Agency (NSTDA) to support Master and Doctoral Degree. Her research area is computational fluid dynamics.

B. Puangkird was a scholarship student under the Development and Promotion of Science Talents (DPST) project, Thailand, and graduated with the first degree in Physics with honours from Mahidol University. He received his Ph.D. in 2007 in the field of Computational Rheology from Swansea University, UK. He is now a lecturer at the Department of Mechanical Engineering, Faculty of Engineering, King Mongkut's Institute of Technology Ladkrabang (KMITL), Bangkok, Thailand. His research is focusing on applied rheology into the fields of food and medical science. It is including computation techniques in the field of mechanics of solids.

V. Ngamaramvaranggul is Assistant Professor of Applied Mathematics at Department of Mathematics and Computer Science, Faculty of Science, Chulalongkorn University in Bangkok, Thailand, one of the world's leading technology university. She's a lecturer of both Mathematics and Computer Science. In 2000, she was awarded her PhD in Computer Science from the Swansea University under the scholarship from the Ministry of University Affairs. Her research includes the computing of fluid dynamics especially for free surface flows and slip conditions. She had ever been a managing director of APAN (Asia-Pacific Advanced Network) Secretariat since 2007-2009.